Int. J. Heat Mass Transfer. Vol. 11, pp. 491–508. Pergamon Press 1968. Printed in Great Britain

ON THE IGNITION AND EXTINCTION PROBLEMS IN FORCED CONVECTION SYSTEMS

V. K. JAIN and H. S. MUKUNDA

Department of Aeronautical Engineering, Indian Institute of Science, Bangalore, India

(*Received* 18 *January* 1967 *and in revised form* 11 *September* 1967)

Abstract—In this paper the problem of ignition and extinction has been formulated for the flow of a compressible fluid with Prandtl and Schmidt numbers taken as unity. In particular, the problems of (i) a jet impinging on a wall of combustible material and (ii) the opposed jet diffusion flame have been studied. In the wall jet case, three approximations in the momentum equation namely, (i) potential flow, (ii) viscous flow, (ii) viscous incompressible with $k = 1$ and (iii) Lees' approximation (taking pressure gradient terms zero) are studied. It is shown that the predictions of the mass flow rates at extinction are not very sensitive to the approximations made in the momentum equation. The effects of varying the wall temperature in the case (i) and the jet temperature in the case (ii) on the extinction speeds have been studied. The effects of varying the activation energy and the free stream oxidant concentration in case (ii), have also been investigated.

NOMENCLATURE

a, coefficient in the potential flow expression $u_e = ax$, representing the characteristic time of the flow [s^{-1}];

c, specific heat at constant pressure [cal/g degK];

D, diffusion coefficient of gas [cm^2/s];

D_1, first Damköhler number defined as $\equiv Z\rho_e/(k+1)a$;

E, activation energy for the reaction [cal/g mol];

$\bar{f}_w$, wall injection parameter defined by equation (30a);

F, the conserved property;

G, mass burning rate per unit area of the mixture [g/cm^2s];

h, total specific enthalpy of the mixture [cal/g];

H, heat of combustion of the fuel [cal/g fuel];

k, constant = 0 for two dimensional flows and = 1 for axisymmetric flows;

K, gradient at the origin $= -(dm_{ox}/dF)_{F=0}$;

L, operator $\equiv \rho u\,\partial/\partial x + \rho v\,\partial/\partial y$;

$\tilde{m}_{fu}, \tilde{m}_{ox}$, non-normalized concentrations of fuel and oxidant;

m_{fu}, m_{ox}, normalized concentrations of fuel and oxidant;

p, pressure [atm];

P, variable defined as $\equiv \tilde{m}_{fu} - \tilde{m}_{ox}/r$;

Pr, Sc, Prandtl and Schmidt numbers;

r, stoichiometric ratio of the fuel;

R, universal gas constant [1·986 cal/g mol degK];

r_0, radius of curvature of the body;

$\tilde{T}$, temperature of the gas [°K];

T, nondimensional temperature;

x, y, coordinates used, as indicated in Figs. 1(a) and 1(b);

u, v, velocities in the directions of x and y;

$\dot{w}_{ox}, \dot{w}_{fu}$, mass rate of production of oxidant and fuel per unit volume [g/cm^3 s];

Z, reaction rate constant in the equation (24) [cm^3/g s].

Greek symbols

β, percentage of oxygen in air;

ξ, η, coordinates of the similarity hypo-

thesis defined by equations (9) and (10);
λ, μ, thermal conductivity [cal/cm s degK] and viscosity of the gas [g/cm s];
ρ, density of the gas [g/cm^3];
φ, equivalence ratio defined in the text;
χ_w, parameter defined by equation (34).

Subscripts

e, edge of the boundary layer;
$-\infty, \infty$, the quantities at negative and positive infinities respectively;
w, the inter phase or "S" state;
ext, quantities at extinction;
eqm, chemical equilibrium;
frozen, frozen state.

1. INTRODUCTION

THE PROBLEM of ignition and extinction of flames in forced convection systems is of considerable interest. It is of importance in transpiration-cooled systems and in re-entry vehicles where the development of flame due to boundary-layer heating is undesirable and in some cases dangerous. If one could predict the extinction speeds for flames in such systems, it would perhaps be possible to keep the missile in a velocity spectrum beyond the extinction speeds and thus prevent the onset of flames.

Studies of a similar nature on opposed jet diffusion flames will help in the evaluation of chemical kinetic data for fuel–air mixtures, specially those which are difficult to handle in the premixed state.

Some of the early studies on this problem have been reviewed by Fendell [1]. Linan [2] formulated the problem for the flow of a compressible fluid and obtained the extinction condition in a rather approximate manner. Jain [3] considered the problem of transpiration cooling in a ramjet. It was of interest to know whether, for a given set of conditions, flame would extinguish. The study, made with a rather *ad hoc* hypothesis for the fluid mechanical part, revealed that the flame would not extinguish. Fendell [1] considered the problem of ignition and extinction of flames near the stagnation point region, when an axisymmetric jet of oxidant blows from an upstream infinity against a reservoir of fuel. He applied the schematics of inner and outer expansions to obtain the chemically frozen and equilibrium states. The plot of maximum temperature vs. first Damköhler number was used to establish ignition and extinction characteristics.

Recently, Tsuji and Yamaoka [4] have considered the problem of wall jet, both analytically and experimentally. They performed the thin-flame analysis using boundary-layer approximations to obtain the position of the flame and its characteristics. However, it is not possible from their analysis to predict the extinction limit due to the fact that infinite rate chemical kinetics has been used. They also performed experiments on the extinction characteristics in a wind tunnel using a cylinder through which various fuels were injected.

The problem of opposed jet diffusion flame was first treated by Spalding [5]. A theory of fluid mechanics as obtained from the analogue solutions of Leclere (see [5]), was used. An approximate procedure was developed for evaluating the volumetric heat release rates. Some of the conclusions of this theory were later verified by the experimental work of Anagnostou and Potter [6]. Fendell and Chung [7] considered the problem with single step reversible reactions (with varying equilibrium constants). The asymptotic methods were used to obtain the various limits governed by the combination of Damköhler number and equilibrium constant.

In recent times, Chung *et al.* [8] considered the problem more systematically using boundary-layer approximations. A parameter consisting of various characteristics of the flame was developed by which "extinction" state and "no-extinction" state could be distinguished.

In the present paper the problem has been formulated for the case of a compressible fluid

with Prandtl and Schmidt numbers taken as unity. The formulation differs from those of Linan [2] and Chung *et al.* [8] in that the chemical kinetic equation used the independent variable as the conserved property, F and not the similarity variable, η. The use of the coordinate F reduces the range of integration from 0 to 1, which is more convenient to handle numerically; however, alternate procedures like the Euler transformation on the independent coordinate could be adopted. In Section 3 of the present paper, the problem of jet impinging on a wall of combustible material is considered. The model used here is similar to those of [1, 3]. As distinct from [3], realistic fluid mechanical solutions have been obtained and used in the chemical kinetic equation. Further, the present paper considers the effects of different approximations used for the fluid mechanics in the evaluation of extinction conditions.

In Section 4, the problem of opposed jet diffusion flame is studied. It is shown that the potential solution is exact so far as the fluid mechanical part is considered. As distinct from [5], the exact numerical solutions of chemical kinetic equation have been obtained. The effects of varying (i) activation energy, (ii) concentration of oxidant at one end and (iii) jet temperatures on extinction speeds have been studied.

2. THEORY

2.1. *Model flow geometry*

(a) Figure 1(a) illustrates the flow near the stagnation point when a perpendicular jet of air (plane or axisymmetric) impinges on a wall of combustible material.

(b) Figure 1(b) depicts the model of the flow pattern for the case of opposed jets when two opposing streams of fuel and air (of varying equivalence ratios) flow towards each other.

2.2. *Assumptions*

The following assumptions are made in the present analysis:

(i) Reaction is assumed to be single step.

(ii) Schmidt (Sc) and Prandtl (Pr) numbers are taken as unity.

(iii) Fourier's law of heat conduction and Fick's law of diffusion are taken as valid.

(iv) Specific heat at constant pressure is assumed constant.

(v) Controlling region of chemical kinetics lies near the stagnation point.

2.3. *Laminar boundary-layer equations*

The equations of motion and conservation for the flow of a compressible fluid with chemical reactions relevant to the present case can be written as [1, 9, 10];

$$\frac{\partial}{\partial x}(\rho u r_0^k) + \frac{\partial}{\partial y}(\rho v r_0^k) = 0 \tag{1}$$

$$L(u) = -\frac{\mathrm{d}p}{\mathrm{d}x} + \frac{\partial}{\partial y}\left(\mu \frac{\partial u}{\partial y}\right) \tag{2}$$

$$L(c\tilde{T}) = u\frac{\mathrm{d}p}{\mathrm{d}x} + \mu\left(\frac{\partial u}{\partial y}\right)^2 + \frac{\partial}{\partial y}\left(\lambda \frac{\partial \tilde{T}}{\partial y}\right) + \frac{H}{r}\dot{w}_{ox} \tag{3}$$

$$L(\tilde{m}_{ox}) = \frac{\partial}{\partial y}\left(D\rho \frac{\partial \tilde{m}_{ox}}{\partial y}\right) - \dot{w}_{ox} \tag{4}$$

$$L(\tilde{m}_{fu}) = \frac{\partial}{\partial y}\left(D\rho \frac{\partial \tilde{m}_{fu}}{\partial y}\right) - \dot{w}_{fu} \tag{5}$$

$$p = \rho \frac{R}{M} T \tag{6}$$

where L (operator) $\equiv (\rho u\ \partial/\partial x + \rho v\ \partial/\partial y)$; M = average molecular weight; r = stoichiometric ratio of the fuel; r_0 = radius of curvature near the stagnation point $= x$; $k = 0$ for two dimensional flows and 1 for axisymmetric flows.

Using the fact that $\dot{w}_{fu} = \dot{w}_{ox}/r$ and defining $P \equiv \tilde{m}_{fu} - \tilde{m}_{ox}/r$ and $h \equiv C\tilde{T} + u^2/2 + H\tilde{m}_{ox}/r$, the equations (3) and (5) can be replaced by the following two equations:

$$LP = \frac{\partial}{\partial y}\left(\mu \frac{\partial P}{\partial y}\right) \tag{7}$$

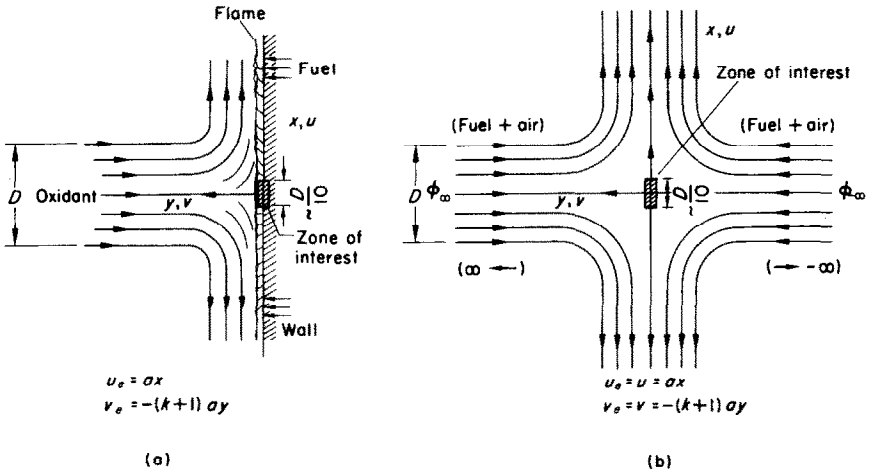

FIG. 1. Schematic diagram of the flow. (a) Wall jet; (b) Opposed jet.

$$Lh = \frac{\partial}{\partial y}\left(\mu \frac{\partial h}{\partial y}\right). \tag{8}$$

In obtaining (7) and (8) we have used the assumption that $Pr = Sc = 1$. It may be noted here that Schvab and Zeldovich (see [1]) were the first to notice that the solution of the three nonlinear equations [equations (3–5)] can be reduced to the solution of (i) two linear equations consisting of diffusive–convective balance of the type (7) and (8) and (ii) one equation involving kinetics of the type of equation (5), *only when* $Pr = Sc = 1$ (this also implies that Lewis–Semenov number is unity). These assumptions ($Pr = Sc = 1$) are valid if the molecular weights of all the species are nearly same. However, for hydrogen–air this is not a good approximation. The case of hydrogen–air has been considered here for the sake of comparison with the results of [3]. Also it is felt that the conclusions of the present paper will not be affected qualitatively by this approximation.

2.4. *Similarity transformations*

The well known Howarth–Dorodnitzyn transformations have been used to obtain a self-similar set of equations. The coordinates ξ and η defined below are introduced:

$$\xi = \rho_e \mu_e a\, x^{2(k+1)}/2(k+1) \tag{9}$$

$$\eta = \left\{\frac{\rho_e a (k+1)}{\mu_e}\right\}^{\frac{1}{2}} \int_0^y \frac{\rho}{\rho_e}\, dy. \tag{10}$$

It may be noted that the equations (9) and (10) have been obtained after introducing, the potential solution near the stagnation point (i.e. $u_e = ax$), into the general Howarth–Dorodnitzyn transformations. The coefficient "a" in the potential solution gives a measure of the characteristic time of the flow (1/s) and depends on the flow geometry. The values of "a" for various flow geometries are tabulated in Table 1.

Table 1

Geometry	Characteristic dimension	a
Cylinder	R = radius of the cylinder	$2u_e$†$/R$
Plane jet (two-dimensional)	h = width of the jet	$\pi \times u_e/4h$
Axisymmetric jet	D = diameter of the jet	u_e/D
Sphere	R = radius of the sphere	$3u_e/2R$

† $u_e = U_{-\infty}$ in the opposed jet case.

Further, introducing the stream function ψ as defined by

$$\rho u x^k = (\partial\psi/\partial y) \text{ and } \rho v x^k = -(\partial\psi/\partial x) \quad (11)$$

and letting further

$$\psi(\xi, \eta) = (2\xi)^{\frac{1}{2}} f(\eta) \quad (12)$$

we obtain the following equations from the system (1–5):

$$(Cf'')' + ff'' + \frac{1}{(k+1)}\left(\frac{\rho_e}{\rho} - f'^2\right) = 0 \quad (13)$$

$$(Ch')' + (fh') = 0 \quad (14)$$

$$(CP')' + (fP') = 0 \quad (15)$$

$$(Cm'_{ox})' + (fm'_{ox}) = \frac{1}{(k+1)a}\frac{\dot{w}_{ox}}{\rho} \quad (16)$$

where $C = (\rho\mu/\rho_e\mu_e)$. The primes in the above equations (13–16) denote differentiation with respect to η. The terms involving derivatives of f, h, P and m_{ox} with respect to ξ do not appear because of the similarity hypothesis.

Introducing a fuel fraction referred to the unburnt state, $\tilde{F}$, we can write the "$\tilde{F}$" conservation equation [5] as

$$(C\tilde{F}')' + f\tilde{F}' = 0. \quad (17)$$

The relationship between F, h and P are given in Sections 3.1 and 4.3.

Further setting $F = \tilde{F}/\tilde{F}_w$, where $\tilde{F}_w$ refers to the value of $\tilde{F}$ at "S" state [3] (interphase state), we obtain the equation (17) as

$$(CF')' + fF' = 0. \quad (18)$$

If $C = 1$, as will be shown later, we obtain

$$F'' + fF' = 0. \quad (18a)$$

The independent variable in the equation (16) can be changed to $\tilde{F}$, using equation (17) to yield:

$$\frac{d^2\tilde{m}_{ox}}{d\tilde{F}^2} = \frac{\dot{w}_{ox}}{(k+1)\rho a C}\frac{1}{(d\tilde{F}/d\eta)^2}. \quad (19)$$

This is the chemical kinetic equation, representing the oxidant conservation. The fluid mechanics enters into this equation through "a" and $(d\tilde{F}/d\eta)$ terms. The former (i.e. a) depends on the potential flow over the given geometry and can be easily determined by analytical or other devices such as electrical analogy tank and conducting paper technique. The latter (i.e. $d\tilde{F}/d\eta$) depends on the numerical solution of the coupled equations (13) and (17) and these being standard equations in compressible flow, solutions are already available for some cases [10, 11]. {The equations (13) and (17) have to be solved for some assumed relations for $C = C(F)$ and $\rho_e/\rho = [\rho_e/\rho]$ (F). For specific cases one should see [10, 11].}

2.5. *Reaction kinetic model*

We assume a reaction rate expression given by

$$\dot{w}_{ox} = Z\rho^{l+m}\tilde{m}_{ox}^{l}\tilde{m}_{fu}^{m}\exp(-E/R\tilde{T}) \quad (20)$$

for a reaction of the type

$$l(\tilde{m}_{ox}) + m(\tilde{m}_{fu}) = n(\text{product}) \quad (21)$$

where Z = rate constant; l, m and n are stoichiometric coefficients of the reaction. We consider in the present paper two reactions, hydrogen oxidation and ethane oxidation:

$$H_2(g) + \tfrac{1}{2}O_2(g) \rightarrow H_2O(g) \quad (22)$$

$$C_2H_6(g) + 3\tfrac{1}{2}O_2(g) \rightarrow 2CO_2(g) + 3H_2O(g). \quad (23)$$

In the present analysis we have used the second order reaction which is both plausible and convenient [1]. The reaction rate expression can then be written as:

$$\dot{w}_{ox} = Z\rho^2\tilde{m}_{ox}\tilde{m}_{fu}\exp[-E/R\tilde{T}]. \quad (24)$$

It is to be noted that in the relations (20) and (24) only forward reactions have been considered and reverse reactions neglected. The reverse reactions become important at very high temperatures. It is felt that the reaction rate expression (24) is adequate for the present study.

Using the reaction rate expression (24) and

the equation of state (6) in the equation (19), we get

$$\frac{d^2\tilde{m}_{ox}}{d\tilde{F}^2} = \frac{Z\rho_e}{(k+1)a}\frac{\tilde{m}_{ox}\tilde{m}_{fu}\tilde{T}_e}{\tilde{T}}\frac{\exp(-E/R\tilde{T})}{C(d\tilde{F}/d\eta)^2}. \tag{25a}$$

After setting $m_{ox} = \tilde{m}_{ox}/\tilde{m}_{ox_e}$, $T = \tilde{T}/\tilde{T}_e$, $m_{fu} = \tilde{m}_{fu}$, $F = \tilde{F}/\tilde{F}_w$ and $T^* = E/R\tilde{T}_e$, we get

$$\frac{d^2m_{ox}}{dF^2} = D_1\frac{m_{ox}m_{fu}}{T}\frac{\exp(-T^*/T)}{C(dF/d\eta)^2} \tag{25b}$$

where

$$D_1 = Z\rho_e/(k+1)a. \tag{26}$$

The parameter D_1 represents the ratio of the characteristic flow time $(1/a)$ to the chemical kinetic time $(1/Z\rho_e)$ and defines the first Damköhler number. It was first introduced by Fendell [1] in connection with the type of problems discussed in this paper. Though this nondimensional number was used in the formulations of Spalding [5] and Jain [3], it was not explicitly recognized so.

Hence the problem boils down to the solutions of the equations (13, 18, 25b) with the appropriate boundary conditions. As the boundary conditions differ because of geometry, they are detailed in the appropriate sections.

2.6. *Scheme of solution*

Equations (13) and (18) have to be solved numerically as simultaneous equations after assuming appropriate relations for C and ρ_e/ρ in terms of F. From these calculations, the profiles of f, F and F' with respect to η are obtained. Then the values of F' at specific intervals of F are interpolated and this information is fed as data while solving the kinetic equation (25b). The solution of the equation (25b) should then reveal the ignition and extinction characteristics. For the numerical solutions of this paper we make the following approximations:

(i) $C = 1$. This implies that $\mu \propto T$. This approximation is found to be generally good in many situations.

(ii) $\rho_e/\rho = 1$ in the momentum equation (13). This implies that the velocity boundary layer is treated as incompressible. This approximation decouples the momentum equation from the conserved property equation and thus leads to considerable simplification in the numerical work. Furthermore, it may be noted that similar approximations have been made in [1, 3, 7].

In the case of wall jet we have obtained some solutions corresponding to the Lees' approximation [8] which amounts to neglecting $(\rho_e/\rho - f'^2)$ term in the momentum equation. A comparison of the solutions obtained using (i) Lees' approximation, and (ii) viscous incompressible approximation with $k = 1$, just noted above, has been made.

3. WALL JET CASE

3.1. *Relationship between m_{ox}, m_{fu}, T and F*

Using the equations (14, 15, 18), we can obtain

$$\frac{h - h_e}{h_w - h_e} = F = \frac{P - P_e}{P_w - P_e} \tag{27}$$

where the subscript w refers to wall or interphase state and e refers to the edge of the boundary layer.

The expressions for m_{fu} and T can be derived in terms of m_{ox} and F using the equation (26) as

$$m_{fu} = \frac{\tilde{m}_{ox_e}}{r}m_{ox} + F\left[\frac{\tilde{m}_{ox_e}}{r} + \left(\tilde{m}_{fu} - \frac{\tilde{m}_{ox}}{r}\right)_w\right] - \frac{\tilde{m}_{ox_e}}{r} \tag{28}$$

$$T = -B\,m_{ox} + F[T_w - 1 + B(m_{ox_w} - 1)] + 1 + B \tag{29}$$

where

$$B = H\tilde{m}_{ox_e}/rc\tilde{T}_e. \tag{29a}$$

It should be noted that the above equations have been obtained after neglecting the kinetic energy term in comparison with chemical and sensible enthalpy terms. As such the present analysis is strictly valid for subsonic velocities inside the boundary layer.

3.2. *Boundary conditions*

(i) On the momentum equation (13).

$$f(0) = \bar{f}_w = (\rho v)_w / \sqrt{[(k+1)\rho_e \mu_e a]} \qquad (30a)$$

where v_w = wall injection velocity of the fuel and $\bar{f}_w$ represents the blowing velocity parameter,

$$f'(0) = 0; \quad f'(\infty) = 1. \qquad (30b, c)$$

(ii) On the conserved property equation (18).

$$F(0) = 1 \quad \text{and} \quad F(\infty) = 0. \qquad (31a, b)$$

(iii) On the kinetic equation (25b).

First we have $m_{ox}(\eta \to \infty) = 1$. The conditions at the wall, however, depend on the type of fuel and are discussed below.

(a) *Gaseous fuel injection.* The conditions at the interphase are obtained using Fick's law as

$$\left(D\rho \frac{\partial \tilde{m}_{ox}}{\partial y}\right)_w = (\rho v \tilde{m}_{ox})_w;$$

$$\left(D\rho \frac{\partial \tilde{m}_{fu}}{\partial y}\right)_w = [\rho v(\tilde{m}_{fu} - 1)]_w. \qquad (32b)$$

These on introducing the transformations yield

$$\left(\frac{dm_{ox}}{dF}\right)_{F=1} = -\chi_w m_{ox_w}; \qquad (33a)$$

$$\left(\frac{dm_{fu}}{dF}\right)_{F=1} = -\chi_w (m_{fu_w} - 1) \qquad (33b)$$

where

$$\chi_w = \bar{f}_w / [C_w F'(0, \bar{f}_w)]. \qquad (34)$$

It is to be noted that $F'(0, \bar{f}_w)$ is obtained by solving for $F(\eta, \bar{f}_w)$ from equations (13) and (18) using the boundary conditions (30a, b, c) and (31a, b).

By using the boundary conditions (33a, b) in the equation (28) we obtain $\tilde{m}_{fuw}$ in terms of $\tilde{m}_{ox_w}$ as:

$$\tilde{m}_{fuw} = \frac{\tilde{m}_{ox_w}}{r} + \left(\frac{\chi_w - \tilde{m}_{ox_e}/r}{1 + \chi_w}\right). \qquad (35)$$

Equation (35) reduces to that obtained in [4] for the thin-flame approximation for which $\tilde{m}_{ox_w} = 0$. We notice that the concentration of fuel becomes negative when

$$\chi_w < (\tilde{m}_{ox_e} - \tilde{m}_{ox_w})/(r + \tilde{m}_{ox_w}). \qquad (35a)$$

It may be noted from the equation (35a) that the injection rate at which $\tilde{m}_{fu_w} = 0$ is less in the case of finite kinetics than in the case of thin-flame theory. The reason for the spurious result that $m_{fu_w} < 0$ for lower injection rates is that if the rates of fuel transfer and of chemical reaction are such that all (or nearly all) the fuel is burned at the interface then the assumption of homogeneous mechanism is violated and the model in the present form is no longer valid. A more general model including heterogeneous reactions at the interface must be considered [4].

(b) *Liquid–solid fuel at the wall (reservoir).* We assume that the wall is at the temperature of boiling–sublimation depending on the type of fuel (liquid–solid). In addition to the conditions (32a, b) we have the condition that the heat transfer at the wall must be sufficient to cause a change of phase from liquid–solid to one of gaseous type. This condition is given by:

$$\left(\lambda \frac{\partial \tilde{T}}{\partial y}\right)_{y=0} = (\rho v \tilde{L})_{y=0} \qquad (36)$$

where $\tilde{L}$ = latent heat of vapourisation–sublimation. On transformation of equation (36), we obtain

$$\left(\frac{dT}{dF}\right)_{F=1} = -L_1 \chi_w \qquad (37)$$

where

$$L_1 = \tilde{L}/c\tilde{T}_e.$$

We now use the equations (33a, b, 35, 37) in the equation (29) to obtain the expression for $\tilde{m}_{ox_w}$ in terms of T_w, L_1 and B as:

$$\tilde{m}_{ox_w} = \frac{1 - T_w + B - L_1 \chi_w}{(H/rC\tilde{T}_e)(1 + \chi_w)}. \qquad (38)$$

Thus the boundary conditions on m_{ox} equation are:

(iii) $m_{ox}(F = 0) = 1$; (39a)

$$\left(\frac{dm_{ox}}{dF}\right)_{F=1} = -\chi_w m_{ox_w}. \quad (39b)$$

In the liquid–solid case, as opposed to gaseous injection case, it is not possible to specify both χ_w and m_{oxw} when other conditions remain unchanged. Therefore, we obtain solutions for the gaseous case for various χ_w, m_{ox_w} and T_w whereas in the liquid–solid case for various χ_w and T_w.

3.3. *Solutions*

(i) *Potential approximation.* It is known that the solution of the momentum equation

$$f''' + ff'' + \frac{1}{(k+1)}(1 - f'^2) = 0 \quad (40)$$

allowing for slip at the wall $[f'(0) \neq 0]$ is

$$f = \eta. \quad (41)$$

This gives the potential velocity distribution near the stagnation point.

Using the solution (41), we solve the equation (18a) under boundary conditions (ii) of Section 3.2 to obtain

$$F = \text{erfc}(\eta/\sqrt{2}) \quad (42)$$

where

$$\text{erfc}(x) = 1 - \text{erf}(x) = 1 - \frac{2}{\sqrt{\pi}}\int_0^x e^{-y^2}\,dy.$$

Therefore,

$$\frac{dF}{d\eta} = -\sqrt{\frac{2}{\pi}}e^{-\eta^2/2}. \quad (43)$$

The numerical procedure adopted to obtain the values of $(dF/d\eta)$ at specific values of F is detailed in the Appendix. The F' vs. F curve for $f_w = 0{\cdot}02$ appears in Fig. 2.

(ii) *Viscous cases*: (*a*) $k = 1$ *and* (*b*) *Lees' approximation.* The equation (40) with $k = 1$ and $k \to \infty$ has to be solved numerically using

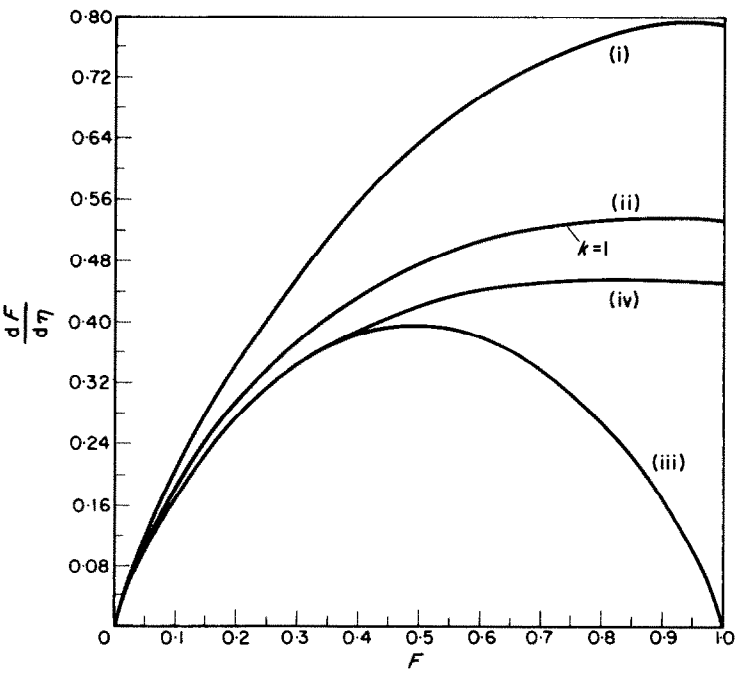

FIG. 2. Plots of $dF/d\eta(=F')$ vs. F. (i) Potential wall-jet: solution of $F = \text{erfc}(\eta/\sqrt{2})$; (ii) Viscous wall-jet: numerical of $ff'' + f''' + (1/k+1)(1-f'^2) = 0$, $F'' + fF' = 0$; (iii) Opposed jet: solution of $F = \frac{1}{2}[1 + \text{erf}(\eta/\sqrt{2})]$; (iv) Wall-jet: viscous, Lees' approximation: numerical solutions of $f''' + ff'' = 0$, $F'' + fF' = 0$.

the boundary conditions (30a, b, c). These solutions have then to be used in (18a) to obtain the solution for F. The details are deferred to the Appendix. The F' vs. F curves for $\bar{f}_w = 0{\cdot}02$ appear in Fig. 2.

(iii) *Numerical solution of equation* (25b). From a thin-flame analysis of the problem it can be shown that for a given fuel, $(dm_{ox}/dF)_{F=0} = -K$, takes extreme values for frozen and chemically equilibrium states. [For frozen flow, $K = 1$ and for chemical equilibrium, $K = \{\chi_w(r + \tilde{m}_{ox_e})/(1 + \chi_w)\tilde{m}_{ox_e}\}$.] Hence to solve the equation (25b) for finite D_1, a value of K lying between the extreme states is chosen and the corresponding D_1 which satisfies the outer boundary condition on m_{ox} is obtained. This is repeated for other values of K. The numerical procedure adopted is detailed below.

The second order nonlinear differential equation (25b) was programmed in Fortran on CDC-3600-160A computer. The Gill modification of Runge–Kutta method was used for the purpose of numerical integration. A step size of 0·01 in F was used in general. Step size control was made depending on the magnitude of the reaction rate term. Step size checks showed that a general step size of 0·01 would lead to values of $(D_1)_{ext}$ within an accuracy of 0·5 per cent. The forward numerical integration was performed by taking the condition on m_{ox} at $F = 0$ and choosing a value of K with a guessed value of D_1. Figure 3 shows the profiles of m_{ox} as D_1 is varied. It is seen that if D_1 is smaller than the correct value, m_{ox} takes negative values at some value of $F > 0$ or at $F = 1$, $(dm_{ox}/dF) > \chi_w m_{ox_w}$. If D_1 is larger than the correct value, m_{ox} profile curls up with successive values of m_{ox} becoming larger or at $F = 1$, $(dm_{ox}/dF) < \chi_w m_{ox_w}$. Using these characteristics, the iteration procedure has been developed. The earlier procedure used by Jain [3] has been modified so that even with a bad initial guess for D_1, convergence to the correct value occurs with relatively smaller number of iterations.

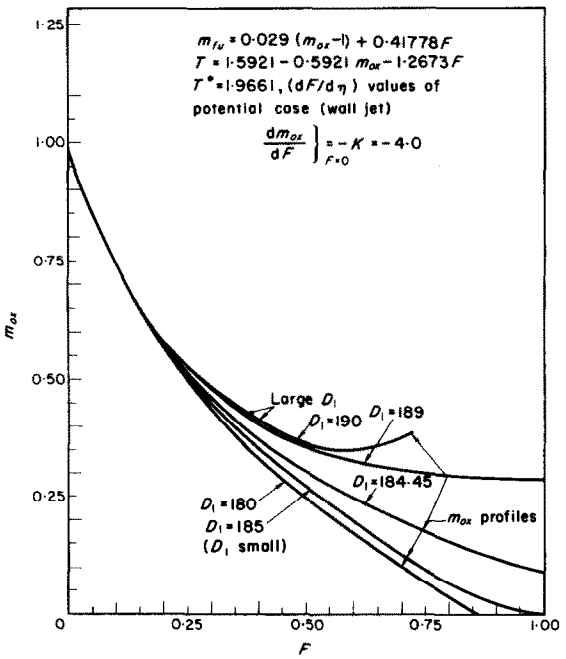

FIG. 3. Variation of oxidant concentration with F (D_1 varying).

3.4. *Results*

(i) In order to check the *ad hoc* hypothesis for the fluid mechanics (of [3]), solutions have been obtained here for (a) the *ad hoc* hypothesis in which $(dF/d\eta)$ is constant throughout, (b) potential velocity field and (c) viscous velocity field $(k = 1)$.

The data used in these calculations are:

$H = 28670$ cal/g hydrogen; $E = 16000$ cal/g mol; $Z = 1{\cdot}381 \times 10^{12}$ cm/gs; $r = 8$; $c = 0{\cdot}24$ cal/g mol degK; $\tilde{T} = 2000°\text{R}$; $T = 7380°\text{R}$; $\rho_e = 0{\cdot}00106$ lb/ft^3; $p = 0{\cdot}178$ atm; $\bar{f}_w = 0{\cdot}25$. The results are compared in Fig. 4.

(ii) The case when jet and wall temperatures are at 300°K was considered to obtain the ignition and extinction characteristics. Further, these calculations have been performed to check the following approximations: (a) potential velocity field, (b) viscous velocity field $(k = 1)$ and (c) viscous: Lees' approximation. These calculations were made on ethane (g) with the following data:

$H = 11350$ cal/g ethane; $E = 35730$ cal/g mol;

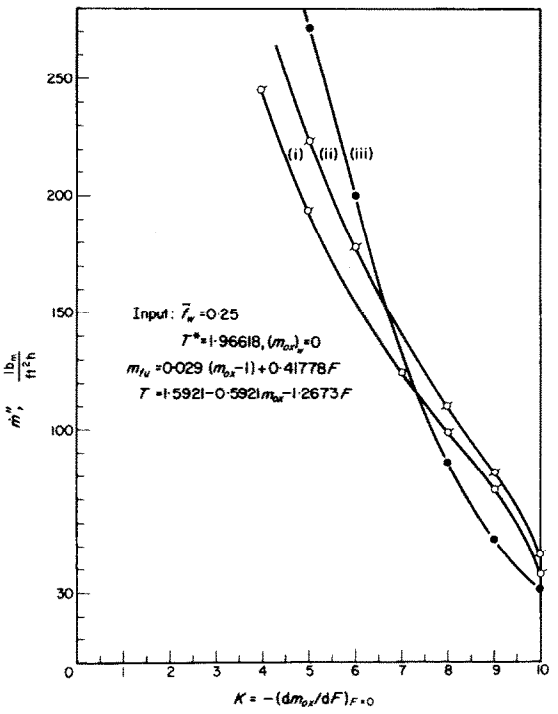

FIG. 4. Comparison of mass flow rates for potential, viscous and Jain's cases. (i) Potential; (ii) Viscous, $k = 1$; (iii) Jain's case: $dF/d\eta$ = constant.

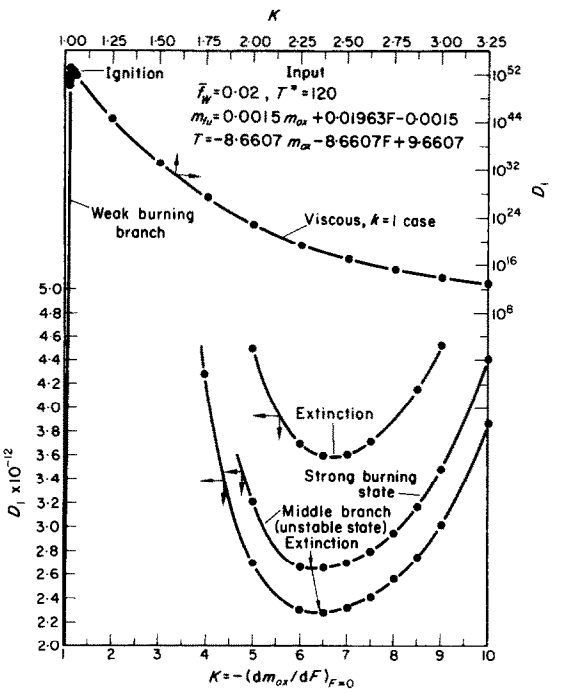

FIG. 5. Plot of D_1 vs. K showing extinction and ignition states.

$\tilde{T}_e = \tilde{T}_w = 300°K$; $r = 3{\cdot}733$; $\bar{f}_w = 0{\cdot}02$; $p_e =$ 1 atm; $\rho_e = 1{\cdot}2$ g/l; $c = 0{\cdot}41$ cal/g degK.

The results are presented in Figs. 5 and 6.

(iii) The temperature of wall ($\tilde{T}_w$) was varied from 300°K to 2400°K and the solutions for extinction conditions for the data of (i) were obtained. The results are seen in Figs. 7 and 8.

4. OPPOSED JET

The equations to be solved are:

$$f''' + ff'' + \frac{1}{(k+1)}(1 - f'^2) = 0 \qquad (44)$$

$$F'' + fF' = 0 \qquad (45)$$

$$\frac{d^2 m_{ox}}{dF^2} = D_1 \frac{m_{ox}\, m_{fu}}{T} \frac{\exp(-T^*/T)}{(dF/d\eta)^2} \qquad (46)$$

where

$m_{ox} = \tilde{m}_{ox}/\tilde{m}_{ox_{-\infty}}$; $T = \tilde{T}/\tilde{T}_\infty$ and $m_{fu} = \tilde{m}_{fu}$.

The boundary conditions are:

(i) On the momentum equation (44).

$$f(0) = 0 \qquad (47a)$$

$$f'(-\infty) = 1 \qquad (47b)$$

$$f'(\infty) = U_\infty / U_{-\infty} \qquad (47c)$$

where U_∞ and $U_{-\infty}$ are the free stream velocities of the jets. In the case of $U_\infty = U_{-\infty}$, by symmetry we obtain another condition:

$$f''(0) = 0. \qquad (47d)$$

(ii) On the conserved property equation (45).

$$F(-\infty) = 0; \quad F(\infty) = 1. \qquad (48a, b)$$

(iii) On the kinetic equation (46).

$$m_{ox}(F=0) = 1; \quad m_{ox}(F=1) = \frac{(\varphi_{-\infty} + r/\beta)}{(\varphi_\infty + r/\beta)} \qquad (49)$$

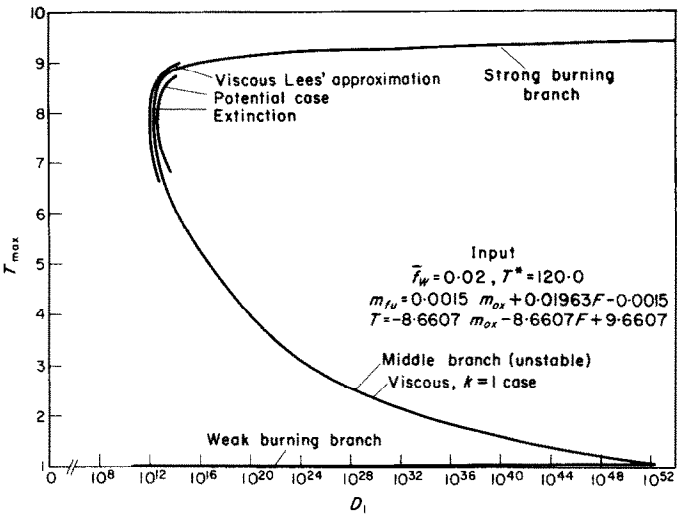

FIG. 6. Plot of T_{max} vs. D_1 showing ignition and extinction states.

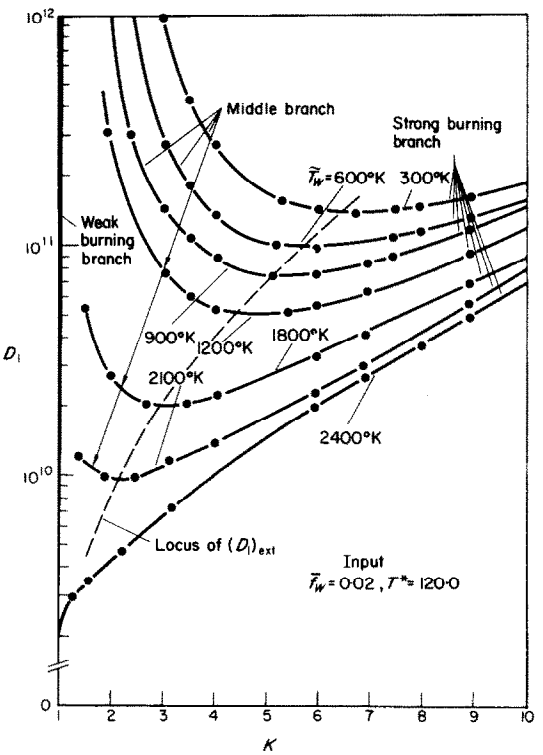

FIG. 7. Variation of D_1 vs. K for various wall temperatures.

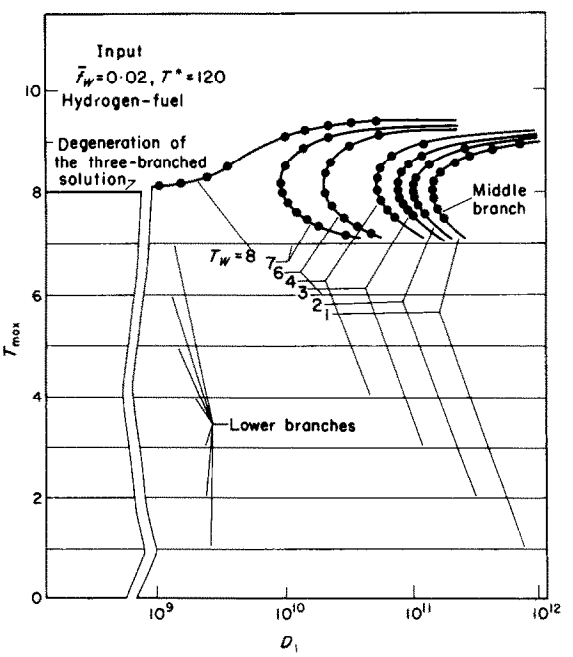

FIG. 8. Variation of T_{max} with D_1 for various wall temperatures.

where φ = equivalence ratio of the streams = (fuel : air)/(fuel : air) stoichiometric,
β = percentage of oxygen in air by weight = 0·232.

4.1. *Relationship between m_{ox}, m_{fu}, T and F*

The relationships between h, P and F are obtained by using the equations (14, 15, 18a) as

$$\frac{h - h_{-\infty}}{h_{\infty} - h_{-\infty}} = F = \frac{P - P_{-\infty}}{P_{\infty} - P_{-\infty}} \tag{50}$$

where

$$F_{-\infty} = 0,\ F_{\infty} = 1 \text{ and } P = \tilde{m}_{fu} - \tilde{m}_{ox}/r.$$

Here, h has been defined in a slightly different way as

$$h = \frac{H\tilde{m}_{fu} + c(\tilde{T} - \tilde{T}_{\infty})}{c(\tilde{T}_b - \tilde{T}_{\infty})} + \frac{u^2}{2} \tag{51}$$

where $\tilde{T}_b$ = burnt temperature.

The equations (50) and (51) can be used to obtain the required relationships between m_{ox}, m_{fu}, T and F as:

$$m_{fu} = \frac{1}{(\varphi_{-\infty} + r/\beta)} m_{ox} + F\left[\frac{(\varphi_{\infty} - 1)}{(\varphi_{\infty} + r/\beta)} - \frac{(\varphi_{-\infty} - 1)}{(\varphi_{-\infty} + r/\beta)}\right] + \frac{(\varphi_{-\infty} - 1)}{(\varphi_{-\infty} + r/\beta)} \tag{52}$$

$$T = -\frac{H}{c\tilde{T}_{\infty}(\varphi_{-\infty} + r/\beta)} m_{ox} + F\left[\frac{H}{c\tilde{T}_{\infty}} \times \left\{\frac{1}{(\varphi_{\infty} + r/\beta)} - \frac{1}{(\varphi_{-\infty} + r/\beta)}\right\} + 1 - T_{-\infty}\right] + T_{-\infty} + \frac{H}{c\tilde{T}_{\infty}(\varphi_{-\infty} + r/\beta)} \tag{53}$$

where

$$m_{ox} = \tilde{m}_{ox}/\tilde{m}_{ox_{-\infty}},\ T = \tilde{T}/\tilde{T}_{\infty}.$$

Again it may be noted that the kinetic energy term has been dropped in the equation (51) while obtaining (52) and (53).

4.2. *Solutions*

(i) *Fluid mechanical solutions.* We consider in the present paper jets of equal diameter and equal velocities. The solution of equation (44) with the boundary conditions (47a, b, d) is then seen to be $f = \eta$. This means that this solution which is incidentally also the potential solution is the exact solution for such a geometry.

(ii) *Conserved property equation* (45). Using the above solution for f in the equation (45), we obtain the solution for F satisfying the boundary conditions (48a, b) as

$$F = \tfrac{1}{2}[1 + \operatorname{erf}(\eta/\sqrt{2})]. \tag{54}$$

so that,

$$\frac{dF}{d\eta} = \frac{1}{\sqrt{(2\pi)}} \exp(-\eta^2/2).$$

The procedure to obtain $(dF/d\eta)$ at desired intervals of F is the same as in Section 3.3.(i). The plot of F' vs. F appears in Fig. 2.

(iii) *Numerical solutions of equation* (46). In the present paper we consider cases when one jet is pure air ($\eta \to -\infty$, $F = 0$) and the other pure fuel ($\eta \to \infty$, $F = 1$). [This means that in the relations (52) and (53), $\varphi_{-\infty} = 0$, $\varphi_{\infty} \to \infty$.] The chemical and thermodynamic data used are the same as in Section 3.4.(ii). The extreme values of K are 1 and $(r/\tilde{m}_{ox_{-\infty}} + 1)$ for frozen flow and chemical equilibrium respectively. The outer boundary condition in the present case is that $m_{ox} = 0$. The numerical procedure is similar to that detailed in Section 3.3.(iii).

Solutions for the case $\tilde{T}_{-\infty} = \tilde{T}_{\infty} = 300°K$ with varying activation energies and oxidant concentrations at one end have been obtained in this paper for ethane–air system. Further in order to study the effects of increasing jet temperatures, the temperatures of both jets were varied from 300°K to 900°K and the results of the increase in extinction velocities are presented in Fig. 10. To study the effect of increasing the temperature of one of the jets, the temperature of the air jet was varied from 300°K to 1200°K, whereas the temperature of fuel jet was kept at 300°K. These results appear in Figs. 11 and 12.

5. DISCUSSION

5.1. *Wall jet case*

(a) *Ramjet problem of* [3]. Figure 4 shows the plots of mass flow rate vs. K for the wall jet case of 3.4.(i). It is seen that the potential approximation underestimates the mass flow rate (in comparison with the viscous case, $k = 1$) by about 10–12 per cent. It is also seen that the *ad hoc* approximation is crude at nearly all gradients except a small region where the two curves intersect [(ii) and (iii) of Fig. 3]. However, the main conclusion of [3] that the flame does not extinguish once it is in a burning state, does not change.

(b) *Comparison of* (i) *potential*, (ii) *viscous*, $k = 1$ *and* (iii) *Lees' approximations.* Figure 5 shows the plot of D_1 vs. K for the three cases mentioned above, following the present approach. In this figure are depicted both ignition and extinction conditions. Following Fendell [1], the T_{max} vs. D_1 curve has also been plotted in Fig. 6. An examination of Figs. 5 and 6 shows that both plots are equivalent in exhibiting the ignition and extinction conditions. The errors in the prediction of mass flow rates of fuel at extinction $(\rho_w v_w)$ are obtained by using the value of $(D_1)_{ext}$ from Fig. 5 in the equation

$$G = (\rho v)_w = \bar{f}_w \rho_e \sqrt{[\mu_e Z/(D_1)_{ext}]}. \qquad (55)$$

The following table gives the mass flow rates at extinction obtained by the three approximations.

	Potential	Viscous, $k = 1$	Lees'
G(g/cm^{2}s)	1·063	1·25	1·35

Taking viscous, $k = 1$ as reference, we see that the Lees' approximation differs by 8 per cent (overestimation) and potential approximation by 15 per cent (underestimation). It thus appears that the results are not affected much by the approximation made in the momentum equation. It is felt, however, that the use of either of the two viscous approximations is preferable to that of potential approximation with regard to the accuracy of the prediction of mass flow rates, although this is yet to be substantiated by comparison with the solution of the exact momentum equation.

(c) *Effect of wall temperature on extinction speeds.* Figure 7 shows the effect of increasing the wall temperature on $(D_1)_{ext}$. The value of $(D_1)_{ext}$ decreases steeply with increase in wall temperature. Taking the values of $(D_1)_{ext}$ at 300°K as reference, we find that the extinction velocity increases by 100 per cent for a temperature increase of 300 per cent. (Note that $D_1 \sim 1/a \sim 1/u_e$.) Further increase in the wall temperature leads to "no extinction" state, i.e. simple transition. It appears that to bring about the "no extinction" state the wall temperature has to be raised to around 2400°K. In this case the three-branched solution degenerates into a single continuous branch. The T_{max} vs. D_1 curves (Fig. 8) reveal the same characteristic. Recently Chung *et al.* [8] proposed a parameter to distinguish the two states, i.e. simple transition–"no-extinction" state and multiple transition–"extinction" state. The parameter written in our notation for the problem is given by:

$$P_c = \frac{(T_{max})_{eqm}}{(T_{max})_{frozen}} \exp\left[-T^*\left\{\frac{1}{(T_{max})_{frozen}} - \frac{1}{(T_{max})_{eqm}}\right\}\right] \times 10^4 \qquad (56)$$

If $P_c \gg 1$, the state corresponds to simple transition. If $P_c \ll 1$, the state corresponds to multiple transition. We see that Fig. 8 demonstrates this qualitatively. The parameter P_c calculated for all the cases in Fig. 7 is tabulated below (Table 2).

It appears that although the parameter P_c exhibits all the qualitative trends properly, the coefficient 10^4 seems large for the present case. It appears that 10^2 is the proper one. However, it is not possible to ascribe a definite value to the coefficient as it will vary from problem to problem.

Table 2. Wall jet case: $\tilde{T}_e = 300°K$, $E = 71560$ cal/g mol, $\tilde{f}_w = 0{\cdot}02$

$\tilde{T}_w$ (°K)	$(T_{max})_{frozen}$	$(T_{max})_{eqm}$ from thin-flame analysis	P_c	Predicted transition as in [8]	Type of transition as from the numerical work (present paper)
300	1	9·376	$2{\cdot}79 \times 10^{-43}$	multiple	multiple
600	2	9·412	$1{\cdot}42 \times 10^{-16}$	multiple	multiple
900	3	9·448	$4{\cdot}64 \times 10^{-3}$	multiple	multiple
1200	4	9·494	$6{\cdot}93 \times 10^{-4}$	multiple	multiple
1800	6	9·556	0·94	multiple	multiple
2100	7	9·592	121·0	simple	simple
2400	8	9·628	952·5	simple	simple

5.2. *Opposed jet diffusion flame*

(a) *Effect of the oxidant concentration on extinction velocity.* In many experimental situations, one uses oxygen or oxygen mixed with varying amounts of nitrogen for the oxidant. It is of interest in such cases to evaluate the effects of varying the concentration of the oxidant. In Fig. 9 is plotted the variation of $U_{ext}/(U_{ext})_{air}$ and $(T_{max})_{ext}$ with $m_{ox-\infty}$. The maximum temperature and the extinction velocity, as expected, increase with increase in oxidant concentration at $-\infty$. This result is in qualitative agreement with the experimental results of Schaffer and Cambel [13] in the case of flame stabilization by opposed jets [vide Fig. 7, p. 286, *Jet Propul.* (1955)]. We can expect neither fair agreement nor very realistic results because the present theory does not take account of heat losses and the realistic reaction kinetics.

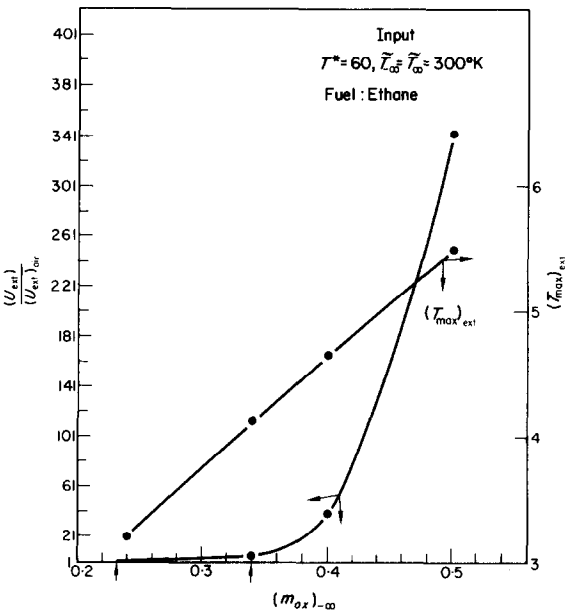

FIG. 9. Effect of variation of oxidant concentration on (U_{ext}) and $(T_{max})_{ext}$.

(b) *Effect of jet temperatures on extinction velocities.* Figure 10 demonstrates the effect of jet temperature on extinction speeds. As in the wall jet case, $(D_1)_{ext}$ decreases with increase in the temperature of the two jets. It is seen that the curves are tending to become flatter and the extinction condition is tending to occur at near frozen states. It is felt that if the temperature were increased still further, the "no extinction" state similar to that obtained in the wall jet case would be obtained.

Figures 11 and 12 show the results for the case when only air jet temperature is increased by keeping the fuel jet at 300°K. It is shown that when jet temperature change is 200 per cent, the extinction speed goes up by 400 per cent. This result is in qualitative agreement with the experimental results of Schaffer and Cambel [13] in the case of flame stabilization by opposed jets.

(c) *Effect of variation in activation energy on extinction speed.* Figure 13, in which activation energy vs. $(D_1)_{ext}$ plot is given, indicates that $(D_1)_{ext}$ varies exponentially with activation energy. This figure can be used to obtain the values of D_1 for various activation energies.

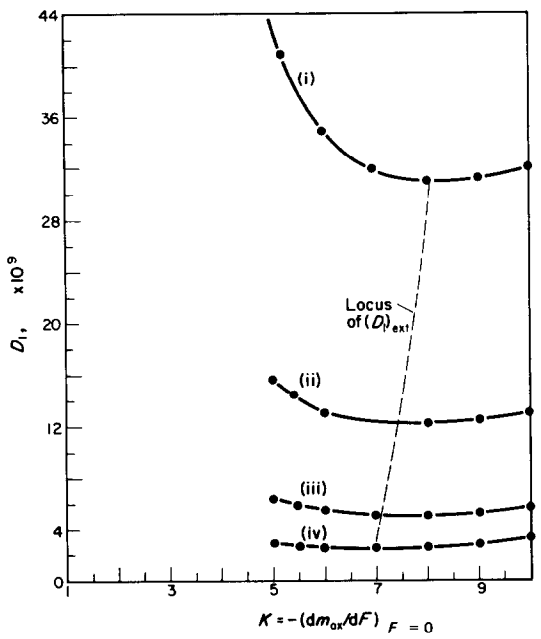

FIG. 10. Effect of the variation of jet temperatures on D_1 ($T_{-\infty} = T_{\infty}$). (i) $\tilde{T} = 300°K$, $T^* = 120$; (ii) $\tilde{T} = 400°K$, $T^* = 90$; (iii) $\tilde{T} = 500°K$, $T^* = 72$; (iv) $\tilde{T} = 600°K$, $T^* = 60$.

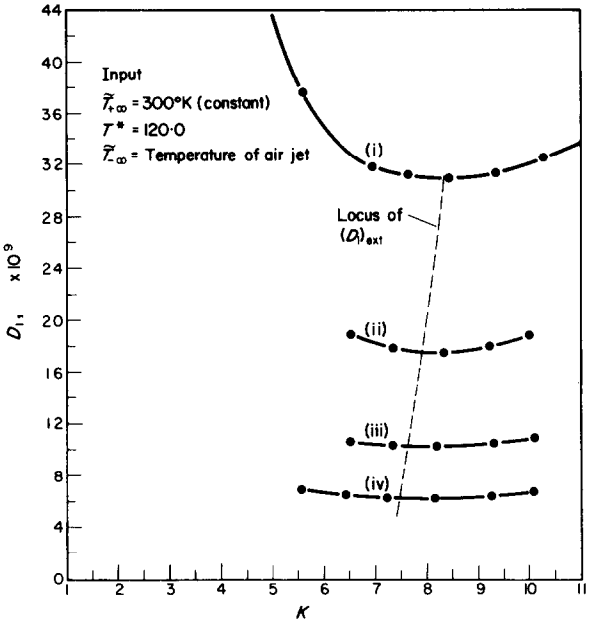

FIG. 11. Variation of Damköhler number with gradient for various air jet temperatures. (i) = 300°K; (ii) = 400°K; (iii) = 500°K; (iv) = 600°K.

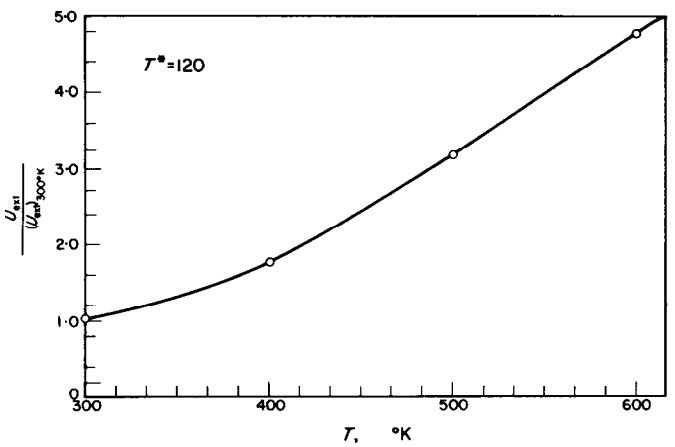

FIG. 12. Variation of extinction speed with temperatures of air jet for the opposed case (hydrogen–air).

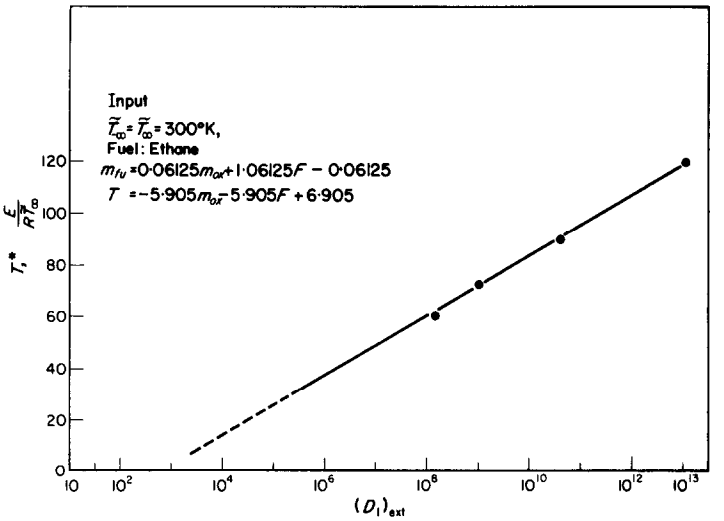

FIG. 13. Effect of variation of activation energy on $(D_1)_{ext}$.

6. CONCLUSIONS

6.1. *Wall jet case*

1. It is shown that the two methods of obtaining ignition and extinction characteristics, (i) by the present method, that of plotting D_1 vs. K and (ii) by Fendell's approach in which T_{max} vs. D_1 plot is used, are equivalent.

2. The prediction of the mass flow rates of fuel at extinction is not very sensitive to the three approximations made in the momentum equation.

3. The extinction speed increases by 100 per cent for a wall jet temperature increase of 300 per cent. Increase in temperature beyond a certain value leads to "no-extinction" conditions.

6.2. *Opposed jet case*

1. The maximum temperature at extinction and the extinction speed increase with increases in the oxidant concentration of the main stream.

2. The extinction speed increases by 400 per cent for an air jet temperature increase of 200 per cent.

3. Increases in the activation energy bring about exponential increases in the values of extinction Damköhler number.

ACKNOWLEDGEMENTS

The authors are thankful to S. S. Krishnamurthy and N. Ramani for their help in programming the problem on the computer. The authors also thank the fluid dynamics group for discussions.

The authors are grateful to the authorities of Tata Institute of Fundamental Research, Bombay, and National Aeronautical Laboratory, Bangalore, for allowing the use of CDC-3600-160A and Ferranti Sirius Computers respectively. The authors are also thankful to the referees for their useful comments. One of the authors (HSM) is grateful to the U.G.C., New Delhi, for the award of Senior Research Fellowship.

REFERENCES

1. F. E. FENDELL, Ignition and extinction on combustion of initially unmixed reactants, *J. Fluid Mech.* **21**, 281–303 (1965).
2. A. LINAN, On the structure of laminar diffusion flames, Ph.D. Thesis, California Institute of Technology, Pasedena (1963).
3. V. K. JAIN, The effects of chemical kinetics on the transpiration cooling of a hypersonic ramjet, Rep. No. IC/HRJ6, Imperial College, London (1962).
4. H. TSUJI and I. YAMAOKA, A gas dynamic analysis of the counter-flow diffusion flame in the forward stagnation region of a porous cylinder, University of Tokyo, Rep. No. 404 (1966); See also Eleventh Symposium (international) on Combustion, University of California, Berkeley (1966).
5. D. B. SPALDING, Theory of mixing and chemical reaction in the opposed jet diffusion flame, *ARS Jl* **31**, 763–771 (1961).
6. E. ANAGNOSTOU and A. E. POTTER, Jr., Flame strength

of propane–air flames at low pressure in turbulent flow, in *Proceedings of the Ninth International Symposium on Combustion*, Vol. 1, Academic Press, New York (1963).
7. F. E. FENDELL and P. M. CHUNG, Combustion of initially unmixed reactants for one step reversible chemical kinetics, Aerospace Corporation Report No. TDR-469 (S5240–10), 1, San Bernardino, California (1965).
8. P. M. CHUNG, F. E. FENDELL and J. F. HOLT, Non-equilibrium anamolies in the development of diffusion flames, *AIAA Jl* **4**, 1020–1026 (1966).
9. L. LEES, Convective heat transfer with mass addition and chemical reactions, in *Combustion and Propulsion, Third AGARD Colloquium*, pp. 451–498. Pergamon Press, Oxford (1958).
10. J. A. FAY and F. R. RIDDELL, Theory of stagnation point heat transfer in dissociated air, *J. Aero/Space. Sci.* **25**, 73–85 (1958).
11. C. B. COHEN and R. RESHOTKO, Similar solution for the compressible laminar boundary layer with heat transfer and pressure gradient, NACA Rep. 1293 (1956).
12. A. CASACCIO, Similar solutions for the laminar mixing of reactive gases, *AIAA Jl* **2**, 1403–1409 (1964).
13. A. SCHAFFER and A. B. CAMBEL, The effect of opposing jet on flame stability, *Jet Propul.* **25**, 284–287 (1955); See also *Jet Propul.* **26**, 576–578 (1956).
14. H. W. EMMONS and D. LEIGH, Tabulation of the Blasius function with blowing and suction, Combustion Aerodynamics Laboratory Interim Technical Report No. 9, Harvard University (1953).

APPENDIX

Inversion of F vs. F′ Relation

(a) We have

$$F = \operatorname{erfc}(\eta/\sqrt{2}) \qquad \text{(A.1)}$$

so that

$$F' = -\sqrt{(2/\pi)}\exp(-\eta^2/2) \qquad \text{(A.2)}$$

The values of F' at specific values of F were obtained by programming the problem on the Ferranti Sirius computer. An approximation for η for a given F was given in (A.1) and the value of η correct to six decimal places was obtained by using the Newton–Raphson procedure of iteration. The value of F' is then easily obtained using equation (A.2).

(b) The solutions of the Falkner–Skan equation for $k = 1$ and $f_w = 0{\cdot}02$ and $0{\cdot}25$ were obtained numerically and the solution of Blasius equation were interpolated using the tables of [14].

The equation $F'' + fF' = 0$ with $F(0) = 1$, $F(\infty) = 0$ was solved by the double quadrature

$$F = 1 - \frac{\int_0^\eta \exp\left(-\int_0^\eta f\,\mathrm{d}\eta\right)\mathrm{d}\eta}{\int_0^\infty \exp\left(-\int_0^\eta f\,\mathrm{d}\eta\right)\mathrm{d}\eta}.$$

From the tabulated values of F and F' at specific values of η, the values of F' at desired intervals of F were interpolated using Lagrange's interpolation formula.

Résumé—Dans cet article, le problème de l'allumage et de l'extinction a été formulé pour l'écoulement d'un fluide compressible avec des nombres de Prandtl et de Schmidt pris égaux à l'unité. En particulier, les problèmes de (1) un jet frappant une paroi de matériau combustible et (2) la flamme de diffusion opposée à un jet ont été étudiés. Dans le cas du jet pariétal, on a étudié trois approximations de l'équation de la quantité de mouvement, c'est-à-dire (1) l'écoulement potentiel, (2) l'écoulement visqueux incompressible avec $k = 1$ et (3) l'approximation de Lees (en supposant nuls les termes de gradient de pression). On montre que les prévisions des flux de masse à l'extinction ne sont pas très sensibles aux approximations dans l'équation de la quantité de mouvement. On a étudié les effets de la variation de la température pariétale dans le premier cas et de la température du jet dans le deuxième cas sur les vitesses d'extinction. Les effets de la variation de l'énergie d'activation et de la concentration en oxydant de l'écoulement libre dans le deuxième cas ont également été étudiés.

Zusammenfassung—Es wird in der Arbeit das Problem des Zündens und Löschens formuliert für den Fall der Strömung eines kompressiblen Mediums der Prandtl- und Schmidt-Zahl Eins. Insbesonders wurden die Probleme (i) des auf die brennbare Wand auftreffenden Strahles und (ii) des gegenläufigen Diffusionsflammstrahles untersucht. Im Fall des Wandstrahles wurden drei Näherungen in der Bewegungsgleichung verwendet, nämlich: (i) Potentialströmung, (ii) zähe Strömung, (ii) zäh, inkompressibel mit $k = 1$ und (iii) Lee's Näherung (wobei die Druckgradienten zu Null genommen werden). Es wird gezeigt, dass die für den Massenstrom beim Löschen errechneten Werte nicht sehr empfindlich von den in die Bewegungsgleichung eingeführten Näherungen abhängen. Der Einfluss veränderlicher Wandtemperatur im Fall (i) und der

Strahltemperatur im Fall (ii) auf die Löschungsgeschwindigkeit wurde untersucht. Die Einflüsse veränderliche Aktivierungsenergie und der Konzentration des Oxidiermittels im Freistrom für den Fall (ii) sind in die Untersuchung einbezogen.

Аннотация—В данной статье сформулирована задача воспламенения и гашения при течении сжимаемой жидкости, при числах Прандтля и Шмидта равных единице. В частности, были исследованы задачи: (1) падения струи на стенку горючего материала и (2) встречных диффузионных пламён. В первом случае рассмотрены три приближения уравнения сохранения количества движения, а именно: (1) потенциальное течение, (2) вязкое несжимаемое течение при $k = 1$ и (3) приближение Ли (где градиент давления принят равным нулю). Показано, что тип аппроксимации уравнения сохранения количества движения не очень сильно влияет на результаты переноса массы при гашении. Исследовано влияние изменяющейся температуры стенки в первом случае и температуры струи во втором случае на скорость гашения. Во втором случае изучено также влияние изменения энергии активации и концентрации окислителя в свободном потоке.